6-2001

Characterizing and Calibrating a Large Helmholtz Coil At Low AC Magnetic Field Levels with Peak Magnitudes Below the Earth's Magnetic Field

Robert A. Schill
University of Nevada, Las Vegas, robert.schill@unlv.edu

Karin V. Hoff
University of Nevada, Las Vegas

Characterizing and calibrating a large Helmholtz coil at low ac magnetic field levels with peak magnitudes below the earth's magnetic field

Robert A. Schill, Jr.
Department of Electrical and Computer Engineering, University of Nevada Las Vegas, 4505 Maryland Parkway, Las Vegas, Nevada 89154-4026

Karin Hoff
Department of Biological Sciences, University of Nevada Las Vegas, 4505 Maryland Parkway, Las Vegas, Nevada 89154-4004

(Received 27 July 2000; accepted for publication 27 February 2001)

Characterizing and calibrating a low impedance large Helmholtz coil generating 60 Hz magnetic fields with amplitudes well below the earth's magnetic field is difficult and imprecise when coil shielding is not available and noise is an issue. Parameters influencing the calibration process such as temperature and coil impedance need to be figured in the calibration process. A simple and reliable calibration technique is developed and used to measure low amplitude fields over a spatial grid using a standard Hall effect probe gaussmeter. These low amplitude fields are typically hard or impossible to detect in the presence of background fields when using the gaussmeter in the conventional manner. Standard deviations of two milligauss and less have been achieved over a spatial grid in a uniform field region. Theoretical and measured fields are compared yielding reasonable agreement for a large coil system designed and built for bioelectromagnetic experiments at the University of Nevada at Las Vegas using simple tools. Theoretical results need to be compared with and adjusted in accord with measurements taken over a large parameter space within the design constraints of the coil. Magnetic field measurements made over a four year period are shown to be consistent. Characterizing and calibrating large Helmholtz coils can be performed with rulers, levels, plumb lines, and inexpensive gaussmeters.
[DOI: 10.1063/1.1368853]

I. INTRODUCTION

The Helmholtz coil has found many applications not suited to other coil systems due to its versatility, ease of accessibility, and relatively uniform field configuration. The Helmholtz coil terminology will be loosely employed here to mean a two coil arrangement sharing the same coil axis lying in planes which are mutually parallel to each other. The coil currents are oriented such that the fields at the geometrical center of the two coil pair add in a constructive manner. The Helmholtz coil terminology is usually reserved for the coil system in which the radius of the coil is directly linked to the distance of separation between the coil plains. Circular and square Helmholtz coils are usually identified with distance of coil separations respectively equal to the coil radius and 0.5445 times the length of the side of the square coil.[1–4] These dimensions provide optimal uniformity over a region. At the cost of a small ripple, the usable region is significantly longer if the coils are spaced somewhat wider than ''Helmholtz.''[5]

Currently, the coil finds applications in bioelectromagnetic experiments,[6–8] in diagnostic studies on electron beams,[9] in the calibration of magnetic instruments and probes,[2,10,11] and in the study of the magnetic properties of materials.[12,13] Some early and present theories have exploited ''on axis'' theories,[14–17] various expansion series,[18–20] and/or approximations[9,10,12,21,22] to examine the magnetic fields generated by current loops as a guide in the design of optimal Helmholtz coils in which the field is nearly uniform over a specified volume. More sophisticated studies have[2,11] or appear to have[23] employed closed form expressions[24–27] for the magnetic fields generated by closed current loops. As echoed in a different work,[11] it is important to obtain the utmost uniformity in the field for sensor and magnetometer calibration. Theory is used as a measure in the design of a Helmholtz coil providing the size and shape of the uniform field region for a given precision.

Low magnitude ac field calibration or characterization over an experimental region in space is not a trivial task. For precise measurements, Helmholtz coils or solenoids are placed in a triaxial Helmholtz coil system (3 m in diameter) which is used to null the background fields at the center of the coil under calibration. A triaxial fluxgate magnetometer is employed to measure the field at the center of the coil system to as low of a value as possible usually less than 1 nT. Then, a proton resonance magnetometer (total field sensing device over the volume of the probe) is used in measuring the fields generated by the coil under calibration supporting a coil current. Residual field effects are minimized by reversing the current in one of the coils after each measurement is taken. At the end of the calibration procedure, the triaxial fluxgate magnetometer is used to measure the changes in the null field at the center of the coil system due to drift. Cancellations of ambient magnetic fields to 4 nT over a 150 mm^3 volume with less than a 1 nT variation over

the volume has been reported.[28] Since the volume of the proton resonance magnetometer is rather large (12 cm long cylinder with a 10 cm diameter in referenced report) a correction in uniformity over the probe is required for most coil systems under test. This correction is significant for small diameter coils.

The experimental procedure conducted by others[28] is of little value when calibrating a large coil since the triaxial Helmholtz coil system needed to nullify the fields must be larger than the coil under test. Further, it is desired to know the field measured in as small a volume as possible about a point in space. If absolute peak ac magnetic field measurements on the order of tens of milligauss (1 μT) and, possibly, milligauss (0.1 μT) are sufficient, a simpler more economical yet nontrivial calibration technique described in this article may be applied with the use of conventional gaussmeters with Hall effect probes. Standard deviations ranging from less than one to two milligauss have been achieved when carefully characterizing the coil over a 12 point spatial grid extending over the uniform field region of the experiment. As indicated in a different work,[11] Helmholtz coils should be considered as the primary standard because they may be calibrated with the use of rulers[11] and, in the case of this effort, rulers, levels, and plumb lines. Approximately 1.5%–2% error in measuring the coil separation and coil radius will begin to yield noticeable field errors on the coil axis.[11] Consequently, measuring large coil dimensions with a ruler is adequate in characterizing the coil.

This effort emphasizes a means to calibrate a Helmholtz coil without the need for high precision equipment. Meaningful spatial measurements are dependent on the accuracy of the measuring devices used and the grid plane in which measurements are taken. Because experimental results are both coil dependent and theory dependent, a detailed design with brief theory is presented. Inaccuracies in the building of the coil as well as coil temperature and impedance will influence the fields being measured. An iterative procedure is used to determine the temperature and coil impedance. Low magnitude ac field measurements are made with conventional gaussmeters driving a Hall effect sensor. These measurements are performed outside of the manufacturer's recommended use of the meter. Stability, repeatability, and drift are examined. Theory and numerical simulation backed up by experimental results over a four year duration show the uniformity of the field over the volume of test. Experimental data extend over an order of magnitude change in field intensity.

In this article, a Helmholtz coil design is presented in Sec. II. Surface plots establishing the theoretical uniformity of the coil fields early on in the design of the coil being characterized are provided. Taking into consideration that the temperature changes in both the coil and current measuring device, an iterative approach is presented on determining the coil resistance. Section III compares experimentally measured fields to theoretical predictions. The process on how experimental data is obtained is carefully documented. A correction factor is determined adjusting the theory to yield a more accurate characterization of the coil.

FIG. 1. Typical setup for calibrating the Helmholtz coil. A level on top of the coil is used to level the planes with respect to gravity. The coil grid with wood block mount containing the gaussmeter probe is shown. In this picture, the probe is mounted at an angle. The plumb bob lines are not visible. The coil with stand is built in a tinker toy fashion and can be partially dismantled. The PVC tube with compression fittings supports both the coil and experiment and is the axis of rotation of the coil.

II. HELMHOLTZ COIL DESIGN

The Helmholtz coil pictured in Fig. 1, was designed from nonmetallic materials outside of the copper winding and coil connectors. A 15/16 in. thick compressed wood composite was used to design the annular rings (1.02 m outer diameter, 0.6 m inner diameter) with an embedded wire winding. Both the type of wood and the wood thickness were chosen to preserve the coil integrity against sagging and warping. The six layers of 12 windings of 18 American wire gauge (AWG) wire were embedded in a centered $\frac{1}{2}$ in. groove about 1 cm deep along the outside perimeter of the annular ring. The groove was coated with boric acid acting as a flame retardant. Wooden dowels and glue anchored the two annular rings to half-meter long wooden supports fixing the overall coil geometry. For mobility purposes, grooves, dovetail joints, and glue were used in the design of the wooden horse stand supporting the coil with experiment. The polyvinyl chloride (PVC) pipe with compression joints attaches the Helmholtz coil to the stand. Further, the PVC pipe located approximately along the secondary axis of the Helmholtz coil supports the experiment. The experiment is contained in a 3 in. diameter, $4\frac{1}{4}$ long glass (400 ml) beaker located at the coil center resting in a hammock style cloth support Velcro to a PVC constructed rectangular structure. The beaker with hammock is not shown. Friction between the wood supports and the pipe axis allows for coil orientation stability. Electrically, the two sets of windings are connected in parallel. The motivation of this electrical configuration is to minimize

the inductance. If the coils are electrically the same, then the current in each set of windings will be of equal amplitude and phase. To examine the electrical properties of each winding set, a 1 Ω resistor (about one fifth of the coil resistance) is connected in series with each winding set in the parallel configuration. A battery operated (electrically and optically isolated) Fluke oscilloscope (dual oscilloscope/meter device) with two channels triggered by one of the channel inputs was used to measure the voltage drop across each resistor. The voltage drops across the 1 Ω resistors when superimposed on top of each other were identical both in magnitude and in phase. Consequently, the currents in each branch are identical. To the two digit accuracy of the meter, the measured electrical resistance of each coil proved identical as well. It is concluded that either a series or parallel coil configuration at least at the 60 Hz frequency is appropriate for this coil system. This is another indication that *large* Helmholtz coils may be constructed with crude instruments and still be reasonable accurate at least at low frequencies. For a 60 Hz source, the largest overall dimension of the coil is many orders of magnitude smaller than the free space wavelength of the 60 Hz wave the source could generate. Further, the overall length of wire in the two sets of windings combined is over two orders of magnitude smaller than a quarter wavelength. Consequently, the phase difference between the upper and lower coils due to some coil perturbation in geometry (such as the exact length of wire used in constructing the coil windings) at this source frequency should be negligibly or unmeasurably small. At higher frequencies (couple of orders of magnitude higher), the electrical equivalence of the two sets of windings must be reexamined.

The Helmholtz coil was designed based on magnetostatics since the largest overall dimension of the coil is small compared to the wavelength of operation. The coil is closely wound. Consequently, the pitch of the individual loops in the coil have been neglected in the theory. The magnetic field components, $b_r(r,z;z')$ and $b_z(r,z;z')$, of a single loop current, I_o,[27] have been computed and added up over the axial directed height of the coil (i.e., the summed effects of the 12 windings in a single layer). Here, z' is the position of the individual loop relative to the central position of the Helmholtz coil along the coil axis. There is less than a 1.3% change in the radius between the first and the sixth winding layer of the coil. Consequently, the magnetic field generated by a wire loop in the sixth layer is nearly equal to that generated by a loop in the first layer. Field corrections due to change in layer radius have been neglected in the theory. This approximation is consistent with an error analysis study.[11] Therefore the coil radius R_o of the first layer is assumed to be the coil radius of the sixth layer. Within the purview of these approximations, the total magnetic field generated by the two coils composing the Helmholtz coil is characterized by

$$B_r(r,z)=\left(\frac{N}{L}\right)\left[\int_{z_{\min}}^{z_{\max}} b_r(r,z;z')dz' + \int_{-z_{\max}}^{-z_{\min}} b_r(r,z;z')dz'\right], \tag{1a}$$

$$B_z(r,z)=\left(\frac{N}{L}\right)\left[\int_{z_{\min}}^{z_{\max}} b_z(r,z;z')dz' + \int_{-z_{\max}}^{-z_{\min}} b_z(r,z;z')dz'\right], \tag{1b}$$

where

$$b_r(r,z;z')=\frac{\mu_o I_o(z-z')}{2\pi r[(r+R_o)^2+(z-z')^2]^{1/2}}\left[\left(1-\frac{k^2}{2}\right)\times\Pi\left(k,-k^2,\frac{\pi}{2}\right)-K(k)\right], \tag{2a}$$

$$b_z(r,z;z')=\frac{\mu_o I_o k}{4\pi[rR_o]^{1/2}}\left[K(k)-\frac{2R_o}{rk^2}E(k) + \frac{-r^2+R_o^2+(z-z')^2}{2r^2}\left(1-\frac{k^2}{2}\right)\times\Pi\left(k,-k^2,\frac{\pi}{2}\right)\right], \tag{2b}$$

$$k^2=\frac{4rR_o}{(r+R_o)^2+(z-z')^2}. \tag{2c}$$

The medium surrounding the Helmholtz coil including the experiment itself is assumed to be nonmagnetic hence the permeability of free space, μ_o, is used. The height of a layer of windings along the coil axis equals the number of turns in a single layer times the diameter of the wire (e.g., 18 AWG wire has a wire diameter of 1.024 mm) given by $|z_{\max}-z_{\min}|$. The distance between the upper coil and the lower coil is $|2z_{\min}|$. The number of turns per unit length along the coil axis is given by N/L. The integral functions $K(k)$, $E(k)$, and $\Pi(k,n=-k^2,\pi/2)$ are, respectively, the complete elliptic integral functions of the first, second, and third kind.

To minimize the size of the Helmholtz coil, a set of design parameters were sought based on numerical simulations of Eqs. (1a) and (1b) on computer for the coil to correct for changes in the magnetic field over the domain of the experiment. Starting at the geometrical center and moving outward, the magnetic field approaches a maximum and then corrects for itself in some directions. This effect is born out in Figs. 2 and 3 for $I_o=1$ A. In Fig. 2 at $z=10$ cm, the radial component of the magnetic field reaches a maximum at roughly $r=5.5$ cm and vanishes at about $r=9$ cm as desired. Over the entire 10 cm radius range, the radial magnetic field varies less than ± 1 mG relative to the desired 0 mG value at the origin. As depicted in Fig. 3 at $r=0$, the axial directed magnetic field gives rise to about a maximum 0.03% change in field at the 6 cm point above (and below) the origin before correcting itself. At $z=\pm 9$ cm, the axial magnetic field is equal to that at the origin. In the $z=0$ plane, the axial directed field monotonically changes by about 0.15% over a 10 cm radial distance from the origin. Theoretically, over a cylindrical volume of 20 cm in length and 10 cm in radius centered at the Helmholtz coil origin with length along the coil axis, an overall maximum change of 3 mG in the radial component and a 0.6% change in the axial component of the magnetic field exit. Over the extent of a 7 cm radius and a 14

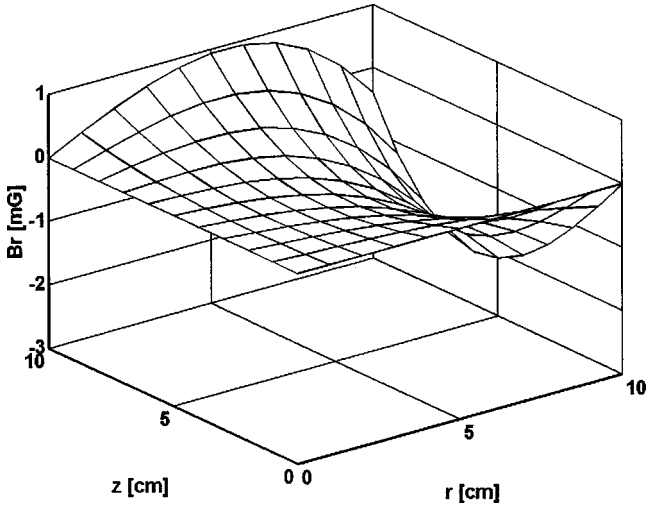

FIG. 2. Numerical simulation of a surface plot of the radial magnetic field over a 10 cm radius and a 10 cm distance in a plane starting along the coil axis (z axis) and origin, respectively. Less than a 3 mG change over the entire surface may be observed. It is interesting to note for this coil design that the field tends to spatially correct itself. This is easily observed along the $z=10$ cm point as the radius of the coil changes from 0 to 10 cm. This tendency is apparent at many cross sections in this figure.

cm in length cylindrical volume positioned about the central point of the Helmholtz coil, there is a 0.9 mG and a 0.15% maximum change in the radial and axial components of the magnetic field, respectively. In both volume regions characterized above, decreasing the coil current by an order of magnitude (i.e., from 1 to 0.1 A) decreases the maximum change in the radial field by an order of magnitude. Both volumes characterized are larger than the size of the glass beaker used to contain the experiment and allows for error in placement of the beaker. Consequently, over the experimental region of test the Helmholtz fields are relatively uniform based on the design theory.

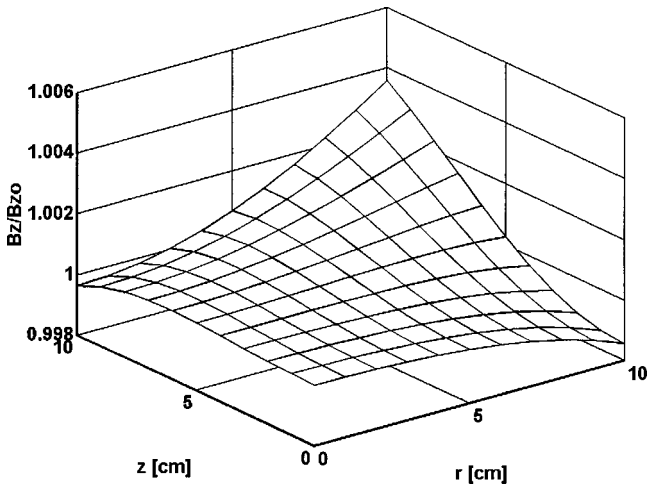

FIG. 3. Numerical simulation of a surface plot of the axial magnetic field (z-directed field) over a 10 cm radius and a 10 cm distance in a plane starting along the coil axis (z axis) and origin, respectively. Less than a 0.007 change in ratio is observed over the entire plane pictured here. It is interesting to note but not easily seen in this figure that for this coil design the field tends to spatially correct itself. The ratio of the field on the z axis with respect to that on the origin is 1. As z increases, the ratio increases to a maximum and then begins to decrease to a value less than 1 as shown in the figure. The magnetic field at the origin for $I_o=1$ A is $B_{z0}=1.274$ G.

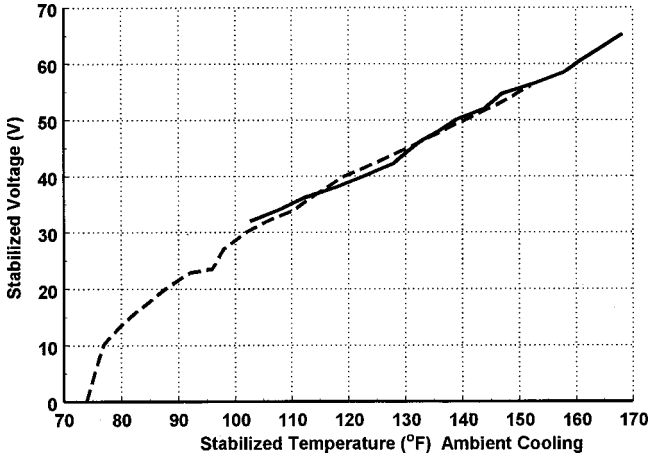

FIG. 4. Steady state temperature of the coil was monitored relative to the voltage applied to the Helmholtz coil by an autotransformer directly connected to a utility outlet. The voltage supplied to the coil was monitored by a Tektronix digital multimeter. Two sets of data taken at different times have been plotted. The ambient Helmholtz coil resistance in parallel configuration is 2.5 Ω.

Figure 4 displays the voltage–temperature characteristics of the Helmholtz coil determined by applying a 60 Hz voltage directly to the Helmholtz coil (in parallel configuration). The temperature was measured from a mercury filled thermometer mounted about 1/8 in. away from one set of windings with bulb embedded in the annular wooden ring. All measurements were taken only after readings were stabilized with time. Figure 4 illustrates that there is no appreciable heating of the coil relative to the ambient temperature (~74 °F) for Helmholtz coil voltages below 10 V ac. Beyond this value, the coil temperature is a strong function of the Helmholtz coil voltage. Over the temperatures of interest, the change in the resistance of each set of windings is linear and is commonly determined by $R(T)=R_1(T=20\,^\circ\mathrm{C})[1+\alpha(T=20\,^\circ\mathrm{C})(T-20\,^\circ\mathrm{C})]$, where $\alpha(T=20\,^\circ\mathrm{C})=0.003\,93$ is the temperature coefficient of resistance for copper at 20 °C, $R_1(T=20\,^\circ\mathrm{C})$ is the resistance of copper at 20 °C, and T is the temperature in degrees celsius of the resistance $R(T)$ to be determined. For 18 AWG wire, the tabulated resistance per unit length and the wire diameter are, respectively, 6.385 Ω per 1000 ft at 20 °C and 1.02 mm. Based on the measured resistance and the relation for wire resistance versus temperature, the Helmholtz coil uses 471.2 m of wire (235.6 m for each set of windings). For voltages below 10 V ac, the ambient (~74 °F) 2.5 Ω Helmholtz coil resistance increases by less than 0.7% and therefore may be considered constant.

Cooled by a muffin fan, the voltage drop monitored across an ambient temperature measured 48.113 Ω resistor (called the ''voltage divider resistor'') in series with the Helmholtz coil is used to determine the coil current. Connecting a 55 V, 60 Hz voltage source across the Helmholtz coil with series resistor caused the resistance of the voltage divider resistor to change by 1.1% of its ambient value yielding a voltage drop of 52.3 V across the resistor. Using the resistance versus temperature expression, Fig. 4 and an iteration technique, the Helmholtz coil resistance increased by

about 0.22% from its ambient value and hence may be assumed to be constant. In the iteration technique, the resistance across each of the two sets of windings is initially assumed to be the cold resistance. Upon calculating the voltage drop across a single winding set, Fig. 4 is used to determine the temperature of the winding set which in turn is used to calculate its new resistance. The procedure is then repeated with the newly calculated resistances until convergence results. It is desired to determine the voltage drop range across the voltage divider resistor that results in less than a 1% change in its ambient resistance. For this purpose, the voltage divider resistance is assumed to change linearly with respect to its voltage drop. As a result, a 1% increase in resistance yields a voltage drop of 47.5 V. Consequently, one may assume that both the voltage divider resistance and the coil resistance are constant when the voltage drop across the voltage divider resistor lies between 0 and 47.5 V. The coil is therefore calibrated over this range.

External metallic mediums may load down the time varying magnetic fields of the Helmholtz coil altering both the amplitude and field structure distributed through the volume of test. A worst case model is examined to determine an upper limit to error resulting from these loading effects. The external medium is modeled as planar, perfect, electrically conducting medium of infinite in extent. Equations (1a) and (1b) are applied using standard techniques of the method of images and superposition to determine the correction to the fields generated at the experiment as a result of the presence of this conducting medium. Excluding both the wire connections to the Helmholtz coil and the experiment itself, all other conducting mediums are contained outside of an imaginary cylinder outlining the Helmholtz coil extending beyond the physical geometry by a coil radius (0.5 m) on all sides. The ratio of the field generated by the planar conductor positioned tangential to this cylindrical shell with unit surface vector perpendicular and parallel to the coil axis relative to the coil generated field is, respectively, 1.2×10^{-2} and 5.5×10^{-2}. The fields generated due to metallic obstacles are less than a factor of 5.5×10^{-2} relative to the coil field in worst case. Over the experimental region, a worst case 6% change in the image field can result due to the planar conductor. Since all conductors are smaller than the infinite perfectly conducting plane and these conductors tend to lie outside of the imaginary bounds, the ratio of the image field to the coil field (without presence of conductor) will be substantially less.

III. EXPERIMENTAL VERSUS THEORETICAL FIELDS: DESIGN CORRECTION FACTOR

Theoretical predictions were compared with experimental data in order to adjust for electrical, mechanical, material, and design errors and theoretical approximations. A model 912 Magnetic Instruments gaussmeter is used to measure the radial and axial magnetic field, generated by the coil, at discrete points in one azimuthal plane over the experimental region. The gaussmeter employed has a three and a half digit accuracy and is not sensitive to measurements below 1 mG. According to the manufacturer's specifications, the meter will provide meaningful measurements of absolute fields as low as 10 mG. The accuracy of 40–400 Hz ac magnetic field readings is plus 1.5% of the reading plus 0.5% of the range. The full scale 10 G range is used in all measurements.

A pegboard mesh doweled to a wooden support mounted on the top of the Helmholtz coil as shown in Fig. 1 provides the grid structure for measurements. Gravity and a ruler are used to position a center column of peg holes along the coil axis. After leveling the Helmholtz coil with respect to gravity (refer to Fig. 1), the center column is aligned along the axis of rotation of the coil using a plumbed, three point, line of sight method with reference to a taunt, externally supported thread. A plumb line was draped over and centered about each end of the PVC pipe supporting the Helmholtz coil. The reference thread was repositioned to just touch each of the plumb line threads. A center column was identified on the pegboard. A plumb line attached to the upper most row of this column was suspended off and centered along the defined center column such that the plumb line just touched the reference line. Further, the tilt of the pegboard plane was adjusted such that the plumb line attached to the pegboard just grazed the pegboard surface. When the center was properly lined up with the reference line, a ruler was used to position the pegboard surface on the geometrical center of the Helmholtz coil parallel to the reference line. The identified center column is now aligned with the axis of the coil. The central position of the coil was located midway between the upper coil and the lower coil. It was not necessary for a peg hole to be located at the origin. Nearest neighbor peg holes were spaced 1 in. apart yielding a square grid of holes. The midplane between the two sets of coils lies 1 1/32 in. below the center line of the first row of peg holes. The gaussmeter probe was very sensitive to rotational changes in position and was therefore mounted in a wooden block. This stabilizes the probe allowing for repeatability and ease in measuring the radial and axial fields in the Helmholtz coil geometry. The probe mount was then attached to the pegboard with flexible plastic tubing commonly used in fish aquariums. The wooden block and the flexible tubing are shown in Fig. 1. In this picture, a pencil was taped to the wooden block only as a visual aid in orientation. The probe tip as viewed from the back side of the pegboard is carefully aligned with the center of the peg hole. Knowing that the magnetic field should be either a minimum or a maximum, the flexible plastic tubing was slightly tighten or loosened until the appropriate maximum or minimum was identified at this position.

In order to measure the small ac magnetic fields generated by the coil, the model 912 gaussmeter was first zero adjusted in dc mode using a zero Gauss chamber and then the Hall effect probe was calibrated to the meter. This is the general operation procedure of the gaussmeter as stated in the manufacturer's instructions. The background fields engulfed the small level ac fields generated by coil making magnetic field measurements in ac mode difficult. The procedure was then augmented by near zeroing the gaussmeter with pegboard mounted probe in ac mode to a minimum value. In this way, the gaussmeter acts as a comparator yielding relative instead of absolute measurements with respect to

TABLE I. Uniformity of the measured and theoretical magnetic field over an 8 cm by 8 cm square area for various coil currents. One edge of the square area lies along the coil axis with the lower comer located about 1 in. above the geometrical center of the Helmholtz coil. The cold voltage divider resistance (VDR) is used: 48.113 Ω. Voltage and peak magnetic field averages (Ave) and standard deviations (SD) are provided.

			Experimental results				Theoretical results[a]			
$V_{\text{VDR Ave}}$ (V)	$V_{\text{VDR SD}}$ (V)	$I_{\text{Helmholtz Ave}}$ (mA)	$B_{z\ \text{Ave}}$ (mG)	$B_{z\ \text{SD}}$ (mG)	$B_{r\ \text{Ave}}$ (mG)	$B_{r\ \text{SD}}$ (mG)	$B_{z\ \text{Ave}}$ (mG)	$B_{z\ \text{SD}}$ (mG)	$B_{r\ \text{Ave}}$ (mG)	$B_{r\ \text{SD}}$ (mG)
5.13	0.028	107	⋯	⋯	0.125	0.61	⋯	⋯	−0.0225	0.0201
5.53	0.039	115	51.2	0.82	⋯	⋯	72.7	0.0275	⋯	⋯
24.14[b,c]	0.686	502	378	6.7	2.5	1.1	317	0.12	−0.106	0.095
35.1[c]	0.117	730	558	2	6.6	2.1	462	0.174	−0.154	0.138

[a]Calculations based on average Helmholtz current.
[b]Data set measured 7/16/96.
[c]Voltage measurements across the voltage divider resistor from *both* radial and *z* directed fields data sets are averaged together.

the background in ac mode. Small changes in the field due to the Helmholtz coil can then be easily detected. The dc zero adjust is not necessary but it does provide a baseline to work from. Stable, repeatable, relative (not absolute) measurements were made even when the absolute ac background field amplitude exceeded the applied field amplitude. Repeatability is based on multiple measurements made over a four year period. For each measurement, the gaussmeter was near zero adjusted in ac mode. The minimum value obtained in this adjustment seemed to be obtained each time assuming the probe plug was not jiggled. Drift in the field measurements were never an issue since field errors were always manually near zero adjusted and measurements were taken within a short period of time. Significant sources of error resulted only when there were large changes in ambient temperature or pressure or when the probe plug was not making good contact internal to the meter. The background fields are always measured when the coil is not energized and is subtracted from the fields measured when the coil is energized. It is noted that the manufacturer's general procedure specifically states NOT to zero adjust the gaussmeter in ac mode.

The uniformity of the magnetic field over a single azimuthal plane of dimension $0<r<8$ cm and $0<z<8$ cm as measured from the coil axis and geometrical origin is depicted in Table I. A twelve-point grid was formed over the plane. Over the plane, both theory and experiment indicate that the standard deviation from the mean field is very small relative to the mean field. This implies a high degree of uniformity for a nearly constant source voltage. This uniformity is in agreement with measurements made over four years ago with the same gaussmeter. Absolute comparisons between theory and experiment do vary significantly. Within the validity of the cold resistance approximation, the measured magnetic field of the coil is plotted against the voltage across the voltage divider resistor (resistor in series with the Helmholtz coil) in Fig. 5. Four measurements are made at 5 V increments between 5 and 45 V. The measured values are then fit with a linear curve. Although a high degree of linearity exists, the fitted curve does not pass through zero. Even so, measurements conducted over a four year period agree well with the experimental curve. Weighting theoretical predictions by an overall 1.19 design factor, yields closer agreement between theoretical and experimental results as shown in the figure.

Data was taken at lower voltage levels as well. As shown in Fig. 5, the data at the two volt level tends to deviate from the linear curve toward the zero voltage, zero magnetic field point as expected. This indicates that the linearity of the curve for voltage levels less than two volts is not valid and the theoretical curve with correction is to be used.

IV. VERIFICATION, COMPARISON, AND DISCUSSION

In the calibration procedure above, the coil was always positioned as shown in Fig. 1. Although convenient for calibration purposes, experimental studies required the coil to be twisted 90° about the pipe axis supporting the coil. To demonstrate a consistency in field uniformity and amplitude, the coil field is examined over a circular cross-section of the beaker supported by the pipe axis.

For perspective, the axis of rotation of the coil (white PVC pipes with compression fittings) was aligned with a compass to point in the north–south direction. Consequently, the Helmholtz coil axis lies along the east–west direction. The beaker is in an upright position located at the approximate center of the coil. Figure 6 provides a sketch of the gaussmeter probe in the beaker with relation to magnetic

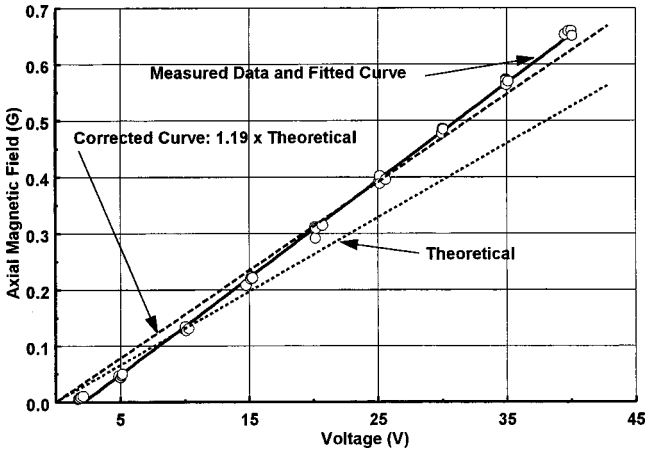

FIG. 5. Theoretical, measured, and corrected axial magnetic field plotted against the voltage measured across a known resistor connected in series with the coil. Note that the experimental data fits along a linear curve that does not pass through the origin. Four data points were taken at 5 V increments. At the 2 V level note that the recorded data begins to deviate from the fitted curve. The position of the probe was fixed on the *z* axis about 1 1/32 in above the geometrical center of the coil.

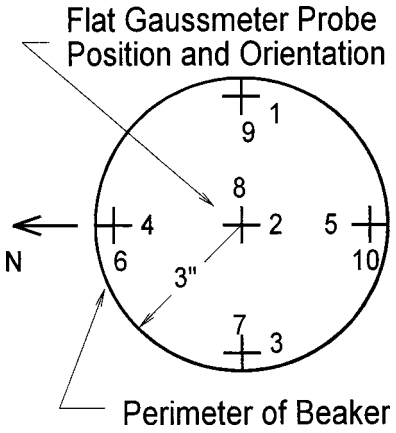

FIG. 6. Sketch of the probe positions inside the region of a beaker in which experiments are conducted. Based on theory and calibration measurements, the exact placement of the beaker at the coil center is not crucial. Allowances have been made in the coil design for the volume of field uniformity to be much larger than the experimental volume actually used.

north as obtained from a compass. A flat one-axis probe was employed for all measurements made in this article. Great care was taken to vertically position the probe and to maintain this exact vertical posture throughout the data recording process. The number associated with the top view silhouette of the probe corresponds to the number found in the position column of Table II. The center of the 3 in. in diameter circular plane in which measurements were taken is located about $1\frac{1}{2}$ in. below the point where the Helmholtz coil axis and the beaker axis intersect lying on the beaker axis. The base of the 3 in. diameter, $4\frac{1}{4}$ in. long (400 ml) glass beaker lies 1 in. below this plane. The surface vector characterizing the plane is parallel to the beaker axis. Two to three measurements were taken at each of the ten probe positions (four perimeter positions and a central position). The average of the difference between the magnetic fields measured in ac mode with the coil current on and with the coil current off is presented in Table II. Measurements were conducted in two

TABLE II. Verification of data measurements with coil in a different orientation. Two cases were examined. In one case a glass beaker located at the approximate center of the coil was empty. In the second case, the glass beaker was filled with water that was allowed to approach room temperature. Two to three sets of data where taken at each probe position for each case. The peak fields were measured. The field reported below is the average (Ave) of the peak fields measured at a probe position in each beaker environment. V_{VDR} is the voltage across the voltage divider resistor.

	Empty beaker		Water filled beaker	
Probe position	$V_{VDR\ Ave}$ [V]	$B_{z\ Ave}$ [mG]	$V_{VDR\ Ave}$ [V]	$B_{z\ Ave}$ [mG]
1	5.28	50	5.35	49
2	5.28	49	5.35	50
3	5.27	49	5.33	49
4	5.31	50	5.39	50
5	5.30	51	5.39	50
6	5.30	0.3	5.38	0
7	5.29	−0.3	5.38	0
8	5.33	−0.3	5.41	1.5
9	5.31	0	5.39	0
10	5.28	−0.3	5.37	0.5

TABLE III. Measured data from Fig. 5 and Tables I and II isolated about 5 V across the voltage divider resistor. Averages (Ave) and standard deviations (SD) of the voltage across the voltage divider resistor (VDR) and the peak amplitude of the axial magnetic field are given.

Source of data	V_{Ave} [V]	V_{SD} [V]	$B_{z\ Ave}$ [mG]	$B_{z\ SD}$ [mG]
Figure 5	5.065	0.112	46.5	2.89
Table I	5.53	0.039	51.2	0.82
Table II (empty beaker)	5.29	0.04	49.8	1
Table II (water filled beaker)	5.36	0.025	49.5	0.5

different environments. In the first case, the beaker was empty and the ambient room temperature was 23 °C. In the second case, the beaker was filled with $2\frac{7}{8}$ in. of tap water. A 26 °C water temperature was measured. In all cases, less than a 3 mG spread in data was observed among measurements taken at a single position for a single environment. The average and standard deviation of both the axial magnetic field and voltage across the voltage divider resistor are given in Table III based on results in Table II. For nearly the same average magnetic field, a 1.3% difference in average voltage across the voltage divider resistor is observed. Consequently, the water filled beaker does not appear to alter the magnetic field amplitudes and its uniformity in a significant fashion. Consequently, loading affects of the beaker with water environment does not significantly distort the low amplitude, 60 Hz, magnetic fields in the experimental region of test. This should be reasonable since the effect of the background fields dominate the orientation of the magnetic dipoles of the water environment. A small perturbation to the field may not significantly alter the properties of this environment. As a result, upon subtracting the background effects, the field information significantly affecting the magnetic and electric properties of the medium is lost at these low amplitudes. Although not recorded here, it is interesting to note that magnetic field measurements taken as the water was quickly approaching the ambient temperature were not stable. It is anticipated that that large temperature changes in the Hall effect sensor influence the sensor operation. Care must be taken in interpreting fields measured when the temperature of the volume under test is not near the ambient temperature.

A significant amount of testing was performed about the 5 V level. Table III summarizes the results gleaned from the data that generated Fig. 5, Table I, and Table II. The average voltage reported in Table II is a result of measurements made for both the axial and radial fields. Table III provides a more accurate representation of the average voltage and standard deviation of only those measurements associated with the axial field data. Since the magnetic field is linearly related to the current and the current is linearly related to the voltage across the voltage divider resistor, then the percent change in voltage across the divider resistor is directly related to the percent change in magnetic field. The data from Fig. 5 is the calibration standard for the coil. Therefore, all comparisons were made with respect to this data. Using the results from Table II, the percent change in average voltage relative to that from the calibrated data when the beaker was empty and water filled is, respectively, 4.54% and 5.82%. Using the standard average axial magnetic field, the projected field for

these respective cases was 48.6 and 49.2 mG. Comparing these values with the average fields obtained from measured data in Table III, very good agreement exists among measured data. Now consider the data in Table III associated with Table I. The percent change in average voltage relative to that from the calibrated data was 9.24%. The projected field is 50.80 mG. The measured field agreed well with the projected field. As observed in the standard deviation of the measured field, the second row of data was taken with care. Each time the probe was repositioned over the grid, the background field reading on the gaussmeter was carefully minimized in ac mode. If the plug of the probe in the gaussmeter box was moved slightly, the minimum background field reading changed as much as 10–20 mG in value and could not be minimized further. Poor internal contact will cause significant errors in all readings. Once the probe plug was firmly pressed into the gaussmeter box so that good electrical contact was made, minimum values obtained in previous measurements were achieved.

In characterizing the Helmholtz coil, one should not be satisfied with measuring the coil fields at one or two coil currents on the axis. Design flaws, coil temperatures, and errors in measuring equipment may provide misleading information when experimental data is coupled to a theory. As in this case, the experimentally generated curve has the same linear tendency as theory but does not pass through the zero magnetic field point when extrapolated to the zero voltage value. Even so, theoretical and experimental results are reasonable so that theoretical results may be fitted to the data and still be forced to pass through the zero voltage–zero field point. This effort verifies that rulers, levels, and plumb lines are satisfactory tools that may be used to calibrate large Helmholtz coils, which is in agreement with a different theoretical study.[11] Even so, every precaution must be taken such that the Hall effect sensor does not twist as measurements are taken from one point to another point on the spatial grid especially when measuring null field components.

ACKNOWLEDGMENTS

M. Bridenburg, R. Sadeghi, and S. Sirin are kindly acknowledged for building the Helmholtz coil illustrated in this article from the first author's design. They were undergraduate students at the time of constructing the coil in 1996. The structure was routed and cut with simple hand tools. Both authors acknowledge both Dr. David Shelton and W. O'Donnell for always being willing to allow us to use their model 912 Magnetic Instruments gaussmeter when needed.

[1] A. H. Firester, Rev. Sci. Instrum. **37**, 1264 (1966).
[2] W. M. Frix, G. G. Karady, and B. A. Venetz, IEEE Trans. Power Deliv. **9**, 100 (1994).
[3] M. E. Rudd and J. R. Craig, Rev. Sci. Instrum. **39**, 1372 (1968).
[4] E. W. Purcell, Am. J. Phys. **57**, 18 (1989).
[5] F. R. Crownfield, Jr., Rev. Sci. Instrum. **35**, 240 (1964).
[6] C. C. Davis, I. Barber, and M. L. Swicord, Bioelectromagnetics (N.Y.) **20**, 203 (1999).
[7] P. Doynov, H. E. Cohen, M. R. Cook, and C. Graham, Bioelectromagnetics (N.Y.) **20**, 101 (1999).
[8] T. Shigemitsu, K. Takeshita, Y. Shiga, and M. Kato, Bioelectromagnetics (N.Y.) **14**, 107 (1993).
[9] R. C. Calhoun, Am. J. Phys. **64**, 1399 (1996).
[10] J. Nissen and L.-E. Paulsson, IEEE Trans. Instrum. Meas. **45**, 304 (1996).
[11] E. L. Bronaugh, IEEE 1995 International Symposium on Electromagnetic Compatibility, Atlanta, Georgia, 14–18 Aug. 1995, p. 72.
[12] S. R. Trout, IEEE Trans. Magn. **24**, 2108 (1988).
[13] P. Murgatroyd, IEEE Trans. Magn. **25**, 2788 (1989).
[14] F. R. Crownfield, Jr., Rev. Sci. Instrum. **35**, 240 (1964).
[15] M. E. Rudd and J. R. Craig, Rev. Sci. Instrum. **39**, 1372 (1968).
[16] E. W. Purcell, Am. J. Phys. **57**, 18 (1989).
[17] P. A. Colavita and V. A. Bustos, Rev. Sci. Instrum. **49**, 1006 (1978).
[18] L. W. McKeehan, Rev. Sci. Instrum. **10**, 371 (1939).
[19] K. Kaminishi and S. Nawata, Rev. Sci. Instrum. **52**, 447 (1981).
[20] M. W. Garrett, J. Appl. Phys. **22**, 1091 (1951).
[21] P. N. Murgatroyd, Am. J. Phys. **59**, 949 (1991).
[22] L. B. Luganskii, Sov. Phys. Tech. Phys. **31**, 537 (1986).
[23] R. K. Cacak and J. R. Craig, Rev. Sci. Instrum. **40**, 1468 (1969).
[24] W. R. Smythe, *Static and Dynamic Electricity*, 2nd ed. (McGraw-Hill, New York, 1950), pp. 270–271, 280–282.
[25] W. R. Smythe, *Static and Dynamic Electricity*, 3rd ed. (Hemisphere, New York, 1989), pp. 290–291, 300–302.
[26] J. Van Bladel, *Electromagnetic Fields* (McGraw-Hill, New York, 1964), pp. 155–156.
[27] R. A. Schill, Jr., IEEE Trans. Magn. (submitted).
[28] J. G. Bartholomew and A. E. Drake, *Proceedings of BEMC '97, 1997 International Conference on Electromagnetic Measurement, Teddington, UK, Nov. 1997* (National Physical Laboratory, Teddington, 1997), pp. 45-1–45-3.